Hindawi
Wireless Communications and Mobile Computing
Volume 2022, Article ID 5326892, 16 pages
https://doi.org/10.1155/2022/5326892

Research Article

RF Fingerprint Extraction Method Based on CEEMDAN and Multidomain Joint Entropy

JianYu Wei, Lu Yu, Lei Zhu, and XingYu Zhou

Institute of Communication Engineering, Army Engineering University of PLA, Nanjing 210000, China

Correspondence should be addressed to Lu Yu; yulu_mail@263.net

Received 11 March 2022; Revised 10 April 2022; Accepted 13 April 2022; Published 10 May 2022

Academic Editor: Mingqian Liu

Specific emitter identification (SEI) can distinguish communication radio emitters with the fingerprint features carried by the received signal, and this technology has been widely used in military and civilian fields. However, in the real electromagnetic environment, the number of communication radio emitters is large and the signal-to-noise ratio (SNR) is low, which leads to poor nonlinear fingerprint analysis of SEI in a single domain. Therefore, combining the exploration of multiple domains of electromagnetic spatial information resources, this paper proposed a radio frequency (RF) fingerprint extraction method based on complementary ensemble empirical mode decomposition with adaptive noise (CEEMDAN) and multidomain joint entropy. The proposed method is an attempt and exploration further extraction of nonlinear fingerprint features in multiple domains. Firstly, considering the nonstationarity of the communication signal, this article adopts the CEEMDAN method to decompose the signal to multiple intrinsic mode functions (IMF). Then, the decomposed signal is represented in multiple spaces by a multidimensional phase space reconstruction technique. Nonlinear analysis of the original signal is performed in multiple spaces: multidimensional differential approximate entropy space, singular spectral entropy space, and power spectral entropy space. Finally, the support vector machine (SVM) is adopted in the classification stage. To demonstrate the robustness of the method, the method is verified on the universal software radio peripheral (USRP) dataset and the Northeastern University public dataset. In terms of the identification accuracy, the proposed method performs with 98.5% accuracy on the 5-class USRP dataset. It also performs with 94.7% accuracy on the 16-class public dataset. The experimental results show that the proposed method has a stable identification performance and has a more than 85% recognition rate in the SNR above 5dB.

1. Introduction

At present, electromagnetic spatial information resources have been elevated to national strategic resources and become one of the high points of the competitive game among contemporary great powers. Specific emitter identification (SEI) is a technique to identify individual radio emitters by extracting external features from a given signal [1], which has great significance in the field of electromagnetic space. The extraction of the fingerprint is the key step of the whole recognition process. The fingerprints of the radio emitter are due to the subtle differences in the production of each unit part of the transmitter such as semiconductors, resistors, and capacitors. Given that RF fingerprinting is unique for each emitter and difficult to fake, the SEI technique plays an important role in military and civil fields, such as battlefield spectrum management [2], and wireless network security [3].

As the fingerprint features of the emitter are affected by various parameter errors such as power amplifiers and frequency sources operating in the nonlinear region, there are many nonlinear components in the modulated signal such as harmonic distortion, transient intermodulation distortion, and cross modulation distortion. Therefore, the modulated signal of the radio emitter is nonlinear and nonstationary actually. We can regard the communication radio emitter as a nonlinear dynamic system, so the problem of fingerprint feature extraction of the radio emitter is

transformed into the problem of nonlinear parameter extraction in a nondynamic system. Carroll [4] creatively proposed that nonlinear dynamic parameters can be extracted from communication radio emitter as a fingerprint for SEI in 2007, and permutation entropy has been well used as an effective nonlinear feature extraction parameter. Normalized permutation entropy [5] extracted from the time-series signal completed the identification of four communication stations. Deng et al. [6] first proposed to use multidimensional entropy to extract an RF fingerprint that differentiates 3 wireless devices with an accuracy of over 93.7%. Xie et al. [7] improved the approximate entropy feature and proposed a differential approximate entropy feature extraction method, which has a good recognition effect on a 3-class task in the low signal-to-noise ratio (SNR). Sun et al. [8] performed nonlinear analysis on multiple wireless network card signals by extracting multidimensional approximate entropy and achieved a high recognition rate of 96.5% in 8 wireless network card signals of the same category. Li et al. [9] first proposed the reverse dispersion entropy (RDE), which not only could capture the subtle changes in the time and frequency domains of the signal but also have better noise robustness. This is beneficial to the mutation signal detection under different SNRs. It can be seen from the above that these methods have a good performance in analyzing the complexity of the waveform and angular structure of the signal in the time domain. Therefore, they obtain high identification accuracy in scenes with high SNR and a small number of individual radio emitters. However, these methods have a common disadvantage; that is, the nonlinear features in multiple domains of the signal are not considered. Due to the existence of multiple individual radio emitters, the difference between their nonlinear fingerprints in a single domain is getting smaller and smaller, and in the low SNR, subtle fingerprint features are easily drowned in noise. Therefore, we need more effective entropy features to represent the nonlinear fingerprint features of radio emitters.

With the development of electromagnetic spatial and temporal big data, information mining, and other technologies, people's understanding of electromagnetic waves gradually changed from the shallow domain (time domain, space domain) to the deep domain (energy domain, singular spectrum domain, and polarization domain). This allows more hidden features to be extracted through the technique of multi-information spatial fusion. In this paper, we propose a novel SEI method and study in the AWGN channel and Rayleigh fading channel. The main contributions are summarized as follows:

(1) We use the CEEMDAN method to extract the high-frequency components of the signal. This method not only helps to remove some environmental noise in the signal but also is beneficial to analyze the subtle features hidden in the signal

(2) Considering the fingerprint feature that exists in the time and frequency domains of the signal from Figure 1, we propose a multidomain joint entropy method to analyze the nonlinear feature in different domains. This method facilitates deep mining of signal fingerprints, which is more adaptable to the realistic complex electromagnetic space

(3) Considering that the nonlinearity of the transmitter and the phase angle structure of the signal are subtle and complex, we propose a multidimensional differential approximate entropy to improve the performance of entropy

(4) To evaluate the noise robustness and the superiority of the proposed method, we compare the performance of the proposed method with other entropy methods in the AWGN channel and Rayleigh fading channel

2. Proposed Feature Extraction Method and Classification

The workflow of this method is shown in Figure 2. First, the received signal is preprocessed, its steady-state part is extracted and segmented, and then, the CEEMDAN method is used to decompose it to obtain multiple intrinsic mode functions. Multidomain joint entropy is extracted from the part IMFs and composes feature vectors which are classified by the SVM in the end.

2.1. CEEMDAN Algorithm. The CEEMDAN algorithm is an improvement to the experience mode decomposition (EMD) algorithm, which is first proposed by [10]. It overcomes the modal aliasing problem in the EMD algorithm, avoids the decomposition error caused by white noise, and reduces the operation cost. It not only has the advantage of multiresolution of the wavelet transform but also overcomes the problem of wavelet base selection. Therefore, CEEMDAN has been widely used in signal processing, especially in dealing with nonlinear and nonstationary signals. The EMD [11] algorithm has serious modal aliasing [12] and end effect [13] phenomena. To suppress the modal aliasing phenomenon, the collective experience mode decomposition (EEMD) [14], the complete ensemble empirical mode decomposition (CEEMD) [14], and the complete ensemble empirical mode decomposition of adaptive noise (CEEMDAN) [15] are successively proposed. CEEMDAN replaces the random white noise with adaptive noise without a basis function [16]. The average residual signal is performed immediately to obtain the individual IMFs, which avoids passing errors to the next iteration. The specific process of the CEEMDAN algorithm is shown as follows:

(1) Defined $\mathrm{IMF}_j(t)(j = 1, 2, \cdots, J)$ is the jth mode obtained by CEEMDAN, and J is the number of the IMF in CEEMDAN. The operator $E_j(.)$ is the j th mode obtained by EMD, $\omega_i(t)\,(i = 1, 2, \cdots, I)$ is the ith added Gaussian white noise, and I is the number of times to add white noise. ε_j is the coefficient of the white noise added to the jth residual component. The ith white noise-added signal $u^i(t)$

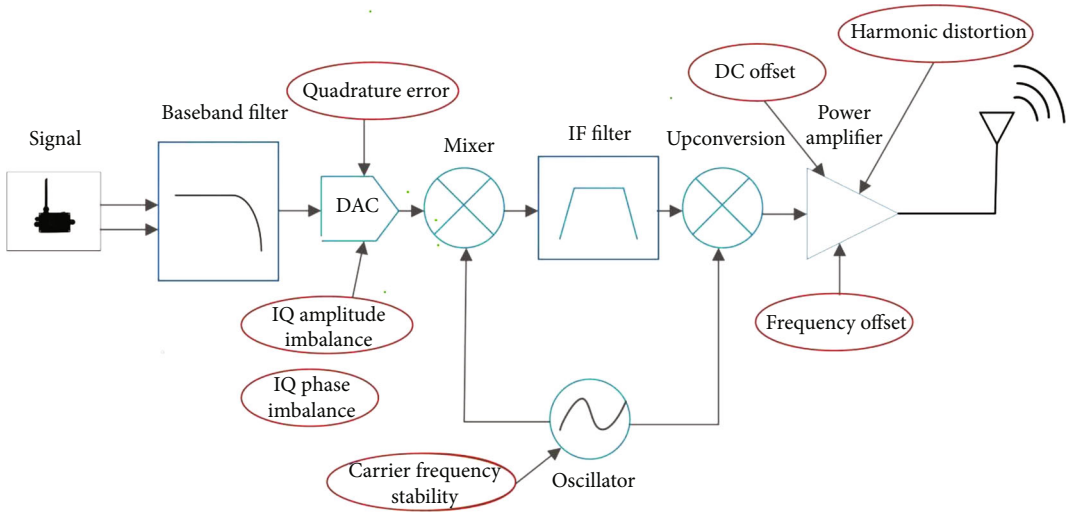

Figure 1: The mechanism of fingerprint generation of radio emitter transmitter.

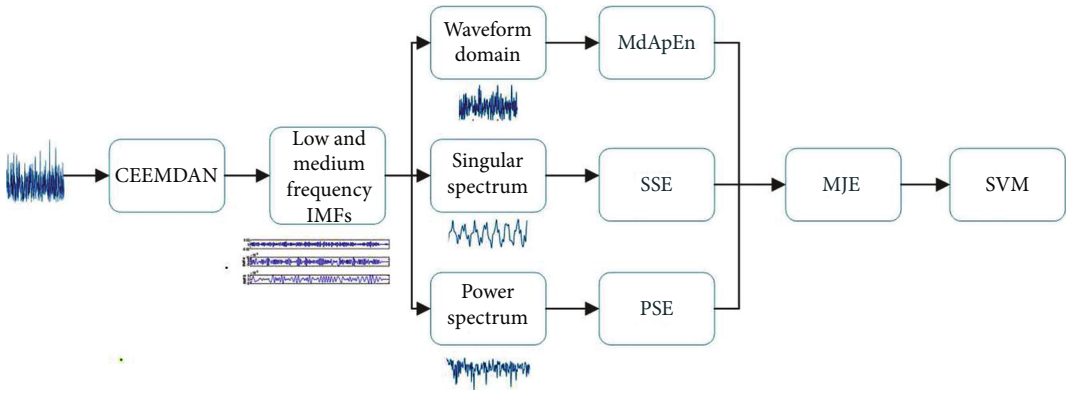

Figure 2: Flowchart of the CEEMDAN-MJE method.

$= u(t) + \varepsilon_0 \omega_i(t)\ (i = 1, 2, \cdots, I)$. Then, the first mode calculated by averaging is

$$\mathrm{IMF}_1(t) = \frac{1}{I}\sum_{i=1}^{I} E_1\left(u^i(t)\right) \tag{1}$$

(2) Define the $r_k(t)$which is the$k$th residual component. Calculating the first residual component is as follows:

$$r_1(t) = u(t) - \mathrm{IMF}_1(t) \tag{2}$$

(3) The signal $r_1(t) + \varepsilon_1 E_1(\omega_i(t))$ is decomposed by EMD. Then, the second mode calculated by averaging is

$$\mathrm{IMF}_2(t) = \frac{1}{I}\sum_{i=1}^{I} E_1\left(r_1(t) + \varepsilon_1 E_1(\omega_i(t))\right) \tag{3}$$

(4) Define the jth signal as

$$r_j(t) = r_{j-1}(t) - \mathrm{IMF}_j(t) \tag{4}$$

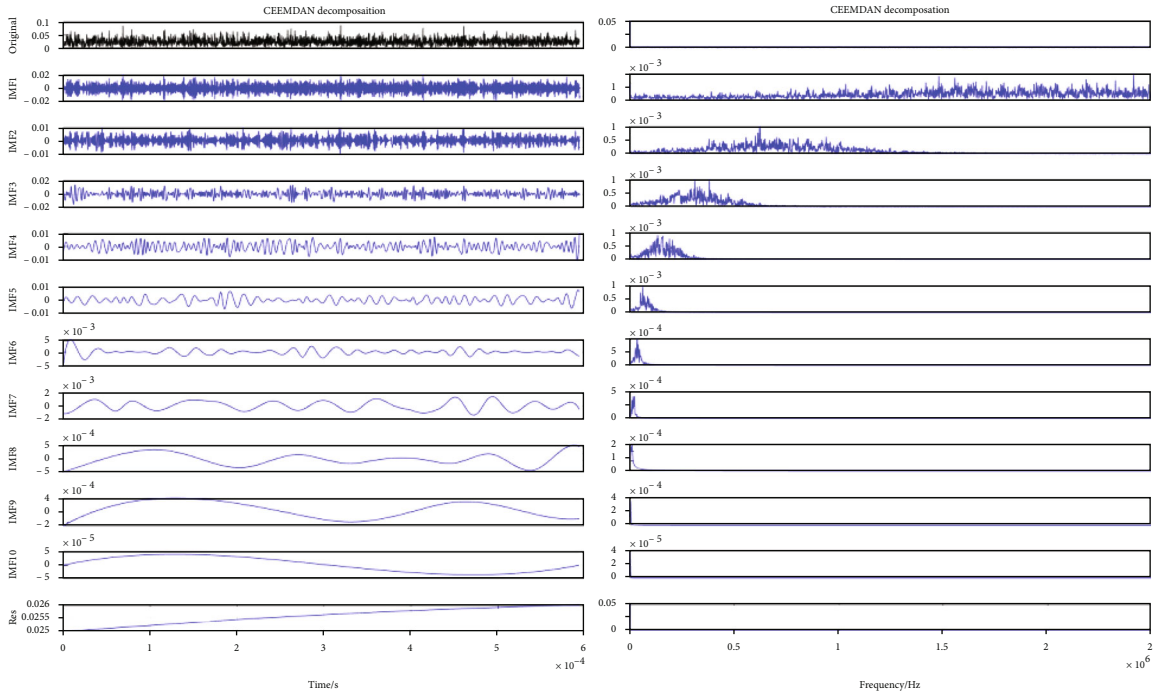

Figure 3: IMFs and spectrum after CEEMDAN decomposition of radio emitter 1.

(5) Decompose the jth signal $r_j(t) + \varepsilon_j E_j(\omega_i(t))$ $(i = 1, 2, \cdots, I)$ by EMD and obtain the jth component. Then, $(j+1)$th mode calculated by averaging is

$$\mathrm{IMF}_{j+1}(t) = \frac{1}{I}\sum_{i=1}^{I} E_1\left(r_j(t) + \varepsilon_j E_j(\omega_i(t))\right) \tag{5}$$

(6) The decomposition process continues until the number of extreme points does not exceed 2, and obtain the residual component $r(t)$. Finally, the signal $u(t)$ is expressed as

$$u(t) = \sum_{j=1}^{J} \mathrm{IMF}_j(t) + r(t) \tag{6}$$

The measured signal $x(t)$ is decomposed by the CEEMDAN algorithm to obtain a series of IMF components from high frequency to low frequency. The CEEMDAN algorithm can separate the different frequency components in the original signal, which is convenient for us to study the features of different frequency parts of the signal. Since the original signal is the sum of these IMF components and the residual, there is no loss of information during decomposition. It can be seen from Figures 3 and 4 that the radio emitter components of IMF2, IMF3, and IMF4 have great differences. Therefore, this paper conducts a nonlinear analysis in different domains for these three components.

2.2. Multidomain Joint Entropy Feature Analysis. In this paper, our innovation is that we propose to extract entropy features in different domains for the first time that represent nonlinear fingerprint features of the communication emitters. These entropy features have been used alone in signal recognition tasks, but this is the first time that they are used jointly. In fact, the nonlinear fingerprint of the signal is subtle and hidden in the waveform of the signal. What is more, according to [17], some fingerprint features have better performance in the frequency domain, such as frequency error, frequency offset, and carrier frequency instability. Therefore, we must use the MJE feature to improve the performance of SEI. In the time domain, we use the MdApEn and singular spectrum entropy (SSE). The MdApEn uses a multiple phase space reconstruction tool to extract features about the phase angle structure. It can represent the fingerprint feature about phase angle in the time domain, such as the IQ phase imbalance. But it pays more attention to the features related to the complexity of the phase angle structure in the time domain of the signal. So we use the singular spectral entropy to further extract nonlinear fingerprint features of the signal. From Figures 5 and 6, the signals of the different emitters have obvious differences in the same singular spectral entropy space. Therefore, the SSE could better reflect fingerprint differences between different emitters. In the frequency domain, the power spectrum analysis method is an effective means to analyze the feature of the signal. Therefore, we use the power spectrum entropy (PSE) to extract the nonlinear

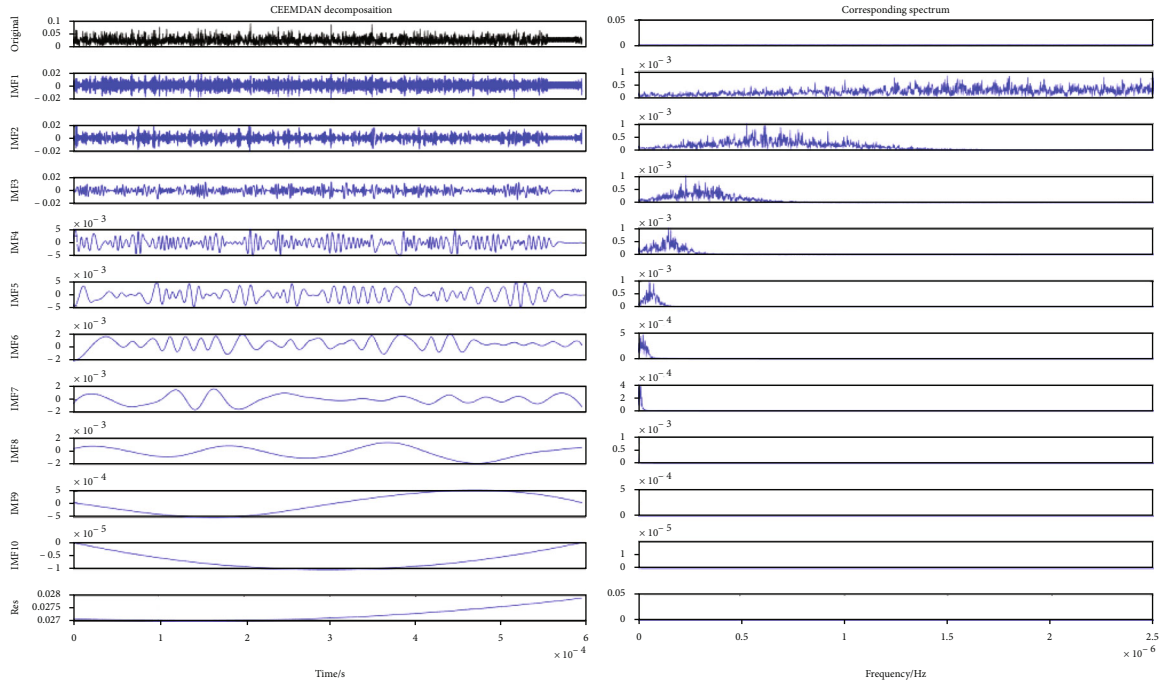

Figure 4: IMFs and spectrum after CEEMDAN decomposition of radio emitter 2.

fingerprint feature in the frequency domain, such as frequency offset and carrier frequency instability. What is more, as we experiment in the paper, the MJE has better performance in the accuracy rate in the lower SNR. Thus, it is important and feasible to use MJE as a feature in SEI.

2.2.1. Multidimensional Differential Approximate Entropy. In the 1990s, Pincus and Huang [18] proposed to use an approximate entropy to measure the complexity of the time series. Considering that the maximum distance method in approximate entropy cannot truly represent the similarity between different signals, Xie et al. [7] proposed the differential approximate entropy algorithm in 2018. They use the differential method to extract the phase angle factor for the discrete sequence of the signal, which can measure the phase similarity between signals. The generation mechanism of nonlinear fingerprint features of communication signals is more complicated, and it is difficult to achieve good results with any of the individual features. Therefore, this paper proposes a method of multidimensional phase space reconstruction to extract the differential approximate entropy of communication signals from different phase spaces. It can reflect the self-similarity of the original sequence more accurately, to calculate the phase angle complexity of the original signal.

Phase space reconstruction is an important tool for analyzing nonlinear signals. After the signal is reconstructed in phase space, more deep features can be extracted in different phase spaces. It is used to map the signal sequences $\{x(i), i = 1, 2, 3 \cdots N\}$ of the communication signal into a multidimensional phase space matrix through the embedded dimension and time delay τ, such as formula (7). Furthermore, the time delay τ is calculated according to the algorithm in [19].

$$X = \begin{bmatrix} x_1 \\ \vdots \\ x_i \\ x_M \end{bmatrix} = \begin{bmatrix} x(1) & x(1+\tau) & \cdots & x(1+(m-1)\tau) \\ \vdots & \vdots & & \cdots \\ x(i) & x(i+\tau) & \cdots & x(i+(m-1)\tau) \\ x(M) & x(M+\tau) & \cdots & x(N) \end{bmatrix}, \tag{7}$$

where $m(m \geq 2)$ is the dimension of the phase space embedding and $M = N - (m-1)\tau$ is the number of time series points in the phase space.

$$x_i = [\, x(i) \quad x(i+\tau) \quad \cdots \quad x(i+(m-1)\tau) \,]. \tag{8}$$

The specific steps of the MdApEn algorithm are as follows:

(1) The time series $\{x(i), i = 1, 2, 3 \cdots N\}$ of the signal are composed to form an m-dimensional vector x_i, $i = 1, 2, 3 \cdots M$

(2) Calculate the corresponding difference term in x_i, which is used to measure the angular structure of the signal sequence:

$$\begin{aligned} xd(i) &= [x(i+\tau) - x(i), \cdots, x(i+(m-1)\tau) - x(i+(m-2)\tau)] \\ &= [t(i), \cdots, t(i+m-2)] \end{aligned} \tag{9}$$

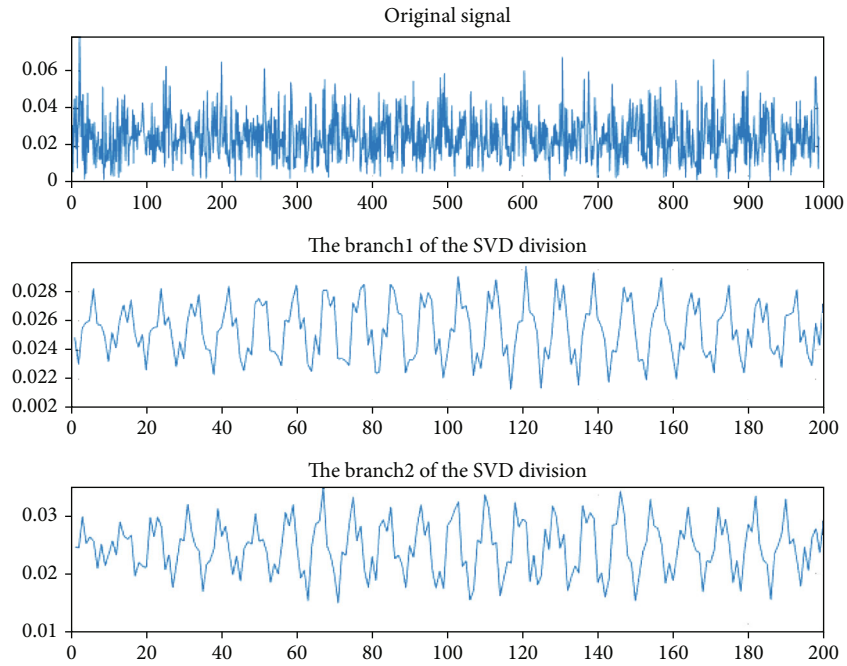

Figure 5: Singular spectral of radio emitter 1.

Define the distance between the different terms $xd(i)$ and $xd(j)$ as

$$d_{ij} = \frac{1}{m-1}\sum_{k=0}^{m-2}|t(i+k) - t(j+k)|. \tag{10}$$

(3) Given a threshold $r(r > 0)$. $\alpha(\alpha > 0)$ is a modified coefficient, and $E\{.\}$ is the mean of the signal $x(n)$:

$$r = \alpha\sqrt{E\{x(n)^2\} - [E\{x(n)\}]^2} \tag{11}$$

(4) Calculate the ratio of the difference item distance $d_{ij} < r$ to the total number of items for each item in $x(i)$, denoted as $C_i^m(r)$:

$$C_i^m(r) = \text{num}\{d_{ij} < r\}/(N - (m-1)\tau) \tag{12}$$

(5) Take the logarithm of $C_i^m(r)$ to calculate the average value, and denote it as $\varphi^m(r)$:

$$\varphi^m(r) = \frac{\sum_{i=1}^{N-m+1}\ln C_i^m(r)}{N - (m-1)\tau} \tag{13}$$

(6) m++, repeat the process from 1 to 4 to get $\varphi^{m+1}(r)$

(7) Calculate differential approximate entropy:

$$H_d(m, r, N) = \varphi^m(r) - \varphi^{m+1}(r) \tag{14}$$

(8) Select the value of m to form a vector; m_i is the ith phase space dimension, which represents the ith embedded dimension of the differential signal:

$$\mathbf{m} = [m_1, m_2 \cdots m_i \cdots m_k] \tag{15}$$

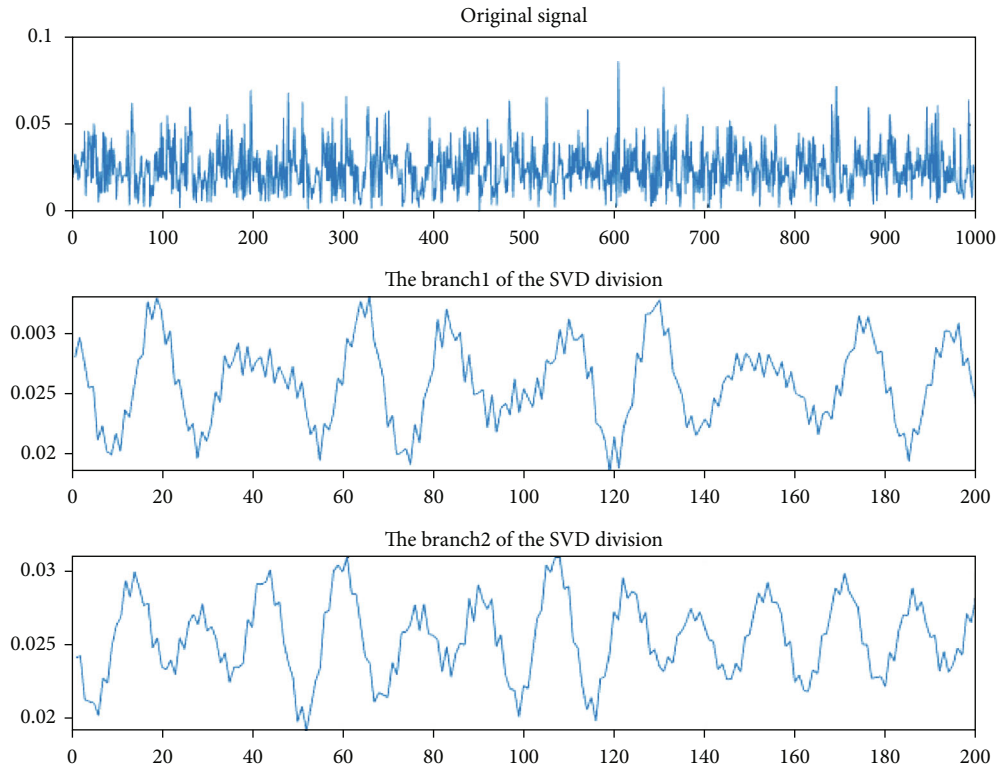

Figure 6: Singular spectral of radio emitter 2.

(9) Calculate the above formula for m_i to get $H_{di}(m_i, r, N)$, denoted as $H_d(m_i)$, which represents the differential approximate entropy of m_i, and normalize it to get

$$H_{di} = \frac{H_d(m_i)}{\ln(m_i!)}, \tag{16}$$

where ! is a symbol for the factorial operation

(10) Obtain the multidimensional differential approximate entropy:

$$H_M = [H_{C1} \cdots H_{Ci} \cdots H_{Ck}] \tag{17}$$

The MdApEn algorithm actually selects signal sequences of different phase spaces for differential processing, so that the corresponding differential terms could be obtained. They enable a more subtle analysis of the changes in the phase angle structure of the signal over a short period of time. The use of the multidimensional makes the analysis of the differential term of the signal more comprehensive. Therefore, it not only more accurately reflects the self-similarity of in the different phase angle structures of the signal segments but also facilitates the deep extraction of the nonlinear fingerprint features of the signal.

2.2.2. Singular Spectrum Entropy. Singular spectrum analysis is a common time-domain analysis method for signals. Its core idea is to reconstruct the time-domain signal and perform singular value decomposition to obtain its inherent complexity features. The singular spectrum entropy [20] essentially reflects the nonlinear features of the time-domain signal under the division of the singular spectrum. From the perspective of signal complexity analysis, it also reflects the energy distribution of the signal in the time domain. The internal inherent feature of the signal and the subtle state changes are also reflected in the time-domain energy distribution, which is closely related to the fingerprint features. As can be seen from Figures 6 and 7, there are subtle differences in the time-domain energy distribution of different communication radio emitters, so the complexity between them is different. Therefore, the singular spectrum entropy of different radio emitter signals has certain differences, and the singular spectrum entropy can reflect the fingerprint features of the signal's time-domain energy distribution to a certain extent.

The specific steps of the SSE algorithm are as follows:

(1) Mapping the discrete signals $\{x(i), i = 1, 2, 3 \cdots N\}$ at point N into the m-dimensional phase space matrix:

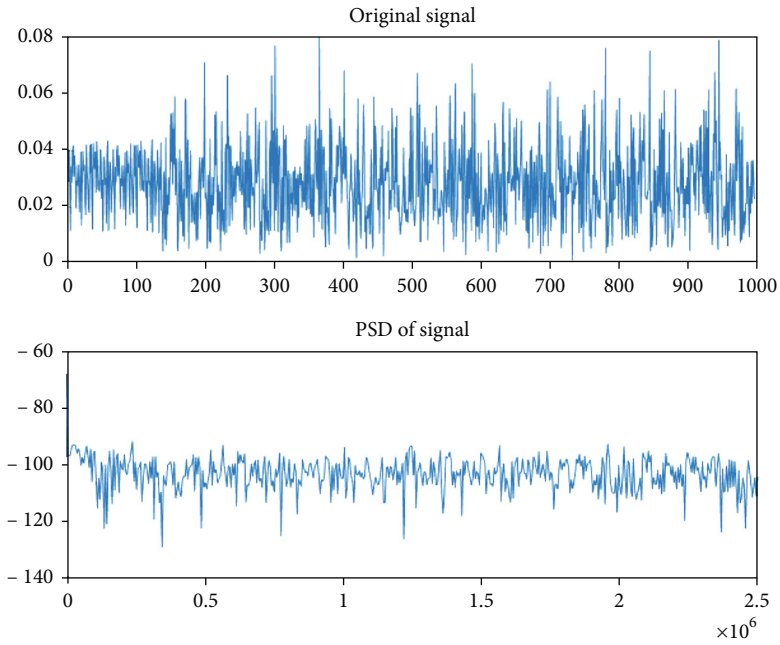

Figure 7: PSD of radio emitter 1.

$$X = \begin{bmatrix} x(1) & x(2) & \cdots & x(M) \\ x(1+\tau) & x(2+\tau) & \cdots & x(M+\tau) \\ \vdots & \vdots & \cdots & \vdots \\ x(1+(\sigma-1)\tau) & x(2+(\sigma-1)\tau) & \cdots & x(M+(\sigma-1)\tau) \end{bmatrix}, \tag{18}$$

where m is the dimension of the phase space embedding; M is generally no more than one-third of the signal length, i.e., $2 \le M \le (N/3)$; τ is the time delay (generally takes the value of 1); and $\sigma = \lceil (N - M + 1)/\tau \rceil$ is the number of time points in the phase space

(2) To decompose the phase space matrix into singular values, let the decomposition obtain m singular values, and arrange all the singular values in order of size to form a sequence $\{\lambda_i (i = 1, 2, \cdots, M)\}$, with $\lambda_1 \ge \lambda_2 \ge \cdots \ge \lambda_M$; then, $\{\lambda_i\}$ constitutes the singular spectrum of the original signal. If the number of nonzero singular values in λ_i is j, the value of j represents the total number of phase spaces contained in the phase space matrix X. And the value of each λ_i reflects the proportion of its corresponding subspace in all phase spaces

(3) From the correspondence between the singular values λ_i and the j subspaces in the phase space matrix X, it follows that the singular spectrum $\{\lambda_i\}$ analysis is a weighting division of the communication signal in the time domain, such that

$$p_i = \frac{\lambda_i}{\sum_{i=1}^{M} \lambda_i}. \tag{19}$$

Then, p_i is the share of the ith singular value in the whole singular spectrum. It also represents the share of the ith subspace in all phase spaces. The singular spectrum entropy of the signal in the time domain can be obtained according to the definition of Shannon entropy as

$$H_s = -\sum_{i=1}^{M} p_i \log p_i \tag{20}$$

(4) Information theory shows that when the entropy takes a great value, the system is in a steady state,

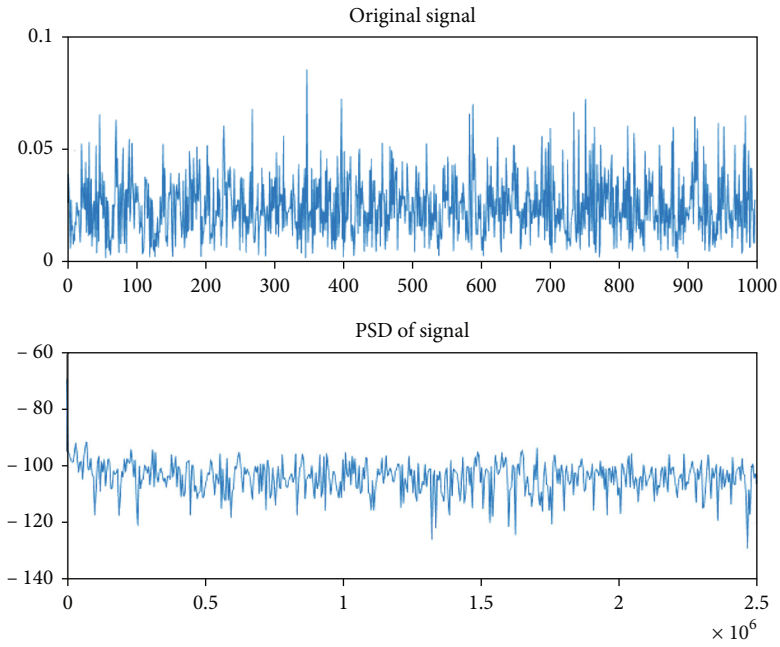

Figure 8: PSD of radio emitter 2.

and the energy distribution is more uniform at this time. And the white noise has the smallest difference in the singular spectrum energy distribution, so its singular spectrum entropy value is the largest, as can be seen from the above equation:

$$H_{S_{\max}} = -M \times \left(\frac{1}{M} \log \frac{1}{M}\right) = \log M. \tag{21}$$

The normalized singular spectral entropy facilitates a more intuitive comparison of signal complexities:

$$\overline{H_s} = \frac{-\sum_{i=1}^{M} p_i \log p_i}{logM} \tag{22}$$

From the perspective of the energy distribution of the signal, it is known that for different radio emitter signals, there is a subtle difference in the energy distribution obtained after its decomposition, and the difference can be effectively indicated through the extraction of a singular spectrum entropy features. From the perspective of signal nonlinear analysis, it can extract and amplify subtle changes in time series, which is closely related to the nonlinear fingerprint feature. Therefore, the singular spectrum entropy can extract the nonlinear fingerprint features of different subspaces under the phase space divided by the singular spectrum and weight by the value of the singular value, which can effectively reduce the influence of noise on the signal.

2.2.3. Power Spectrum Entropy. The fingerprint features and subtle state changes within the signal are often reflected in its frequency composition and changes in the energy distribution in the frequency domain, so spectral analysis of the signal is often more conducive to capturing subtle features that are not obvious in the time domain, and the nonlinear fingerprint features have different performances in the frequency domain. The power spectrum analysis method is an effective means to analyze the signal in the frequency domain.

The power spectrum is the abbreviation of power spectral density function, defined as the signal power per unit frequency band. It reflects the distribution of the signal power in the frequency domain; the uniformity of the power spectrum distribution can represent the complexity of the original signal. As can be seen from Figures 7 and 8, there are subtle differences in the uniformity of the power spectrum distribution of different communication radio emitters. What is more, the fingerprint features affect the uniform distribution of the power spectrum and are reflected in its subtle changes. Therefore, to a certain extent, the power spectrum entropy features can effectively extract the nonlinear fingerprint features of the radio emitter in the power spectrum domain.

The specific steps of the PSE algorithm are as follows:

(1) Discrete Fourier transform of the discrete signal $\{x(i), i = 1, 2, 3 \cdots N\}$ for N points:

$$X(k) = \sum_{n=0}^{N-1} x(n) e^{-j(2\pi/N)nk}, \tag{23}$$

where $k = 1, 2 \cdots N - 1$ is the frequency order

(2) Calculating the power spectrum density, according to the relationship between signal and energy, the

Table 1: Selection results of penalty coefficient c.

c	Ninefold cross-validation									Average
0.01	0.906	0.915	0.838	0.920	0.914	0.953	0.931	0.925	0.953	0.915
0.1	0.971	0.910	0.983	0.982	0.901	0.926	0.928	0.931	0.893	0.936
1	0.978	0.982	0.942	0.954	0.958	0.963	0.944	0.972	0.989	0.964
10	0.988	0.972	0.971	0.991	0.942	0.991	0.983	0.987	0.977	0.978
20	0.970	0.957	0.963	0.955	0.941	0.933	0.890	0.931	0.907	0.938

Table 2: Selection results of parameter gamma.

Gamma	Nine-fold cross-validation									Average
10	0.913	0.889	0.873	0.925	0.841	0.863	0.871	0.916	0.932	0.891
50	0.871	0.940	0.973	0.988	0.951	0.915	0.947	0.901	0.881	0.929
100	0.966	0.985	0.964	0.977	0.979	0.989	0.991	0.872	0.903	0.954
150	0.982	0.989	0.977	0.987	0.982	0.989	0.963	0.957	0.977	0.977
200	0.966	0.967	0.965	0.975	0.987	0.963	0.906	0.958	0.987	0.965

Input: Signal sequences $X(i.)$
Output: Multi-domain Joint Entropy
1. Initialization: M, $\boldsymbol{m}$, r, τ and σ;
2. Get the steady-state part of the signal and the corresponding IMF components are obtained by CEEMDAN decomposition of the signal;
3. From the relevant experience, the frequency distribution of the IMF is selected according to the high and medium frequency components for superposition noted as IMF
4. The multi-domain joint entropy feature is extracted for the IMF and is denoted as:
$\boldsymbol{H} = [H_M, \overline{H_s}, \overline{H_p}]$
5. Classification and recognition of $\boldsymbol{H}$ using SVM Classifier;

Algorithm 1: CEEMDAN-MJE method

power spectrum of each order frequency can be obtained:

$$S(k) = \frac{1}{N}|X(k)|^2 \tag{24}$$

(3) Calculating the power spectrum entropy, the power spectrum of each order frequency is essentially a division of the original signal in the frequency domain, and the total energy of the signal is $1/N$ times the sum of the energy $|X(k)|^2$ of each order frequency component, defining the weights of its power spectrum distribution as

$$q_k = \frac{S(k)}{\sum_{k=0}^{N-1} S(k)} \tag{25}$$

(4) Where q_k is the share of the kth order power spectral component in the whole power spectral components. From the definition of Shannon entropy, the power spectrum entropy is obtained as

$$H_p = -\sum_{i=1}^{N-1} q_k \log q_k \tag{26}$$

(5) When the entropy takes a great value, the system is in a stable state and the power spectrum is the most uniform. The white noise has the smallest difference in the power spectrum energy distribution, so its singular spectrum entropy value is the largest, as can be seen from the above equation:

$$H_{p_{\max}} = -N \times \left(\frac{1}{N} \log \frac{1}{N}\right) = \log N. \tag{27}$$

The normalized power spectrum entropy facilitates a more intuitive comparison of the signal complexity:

$$\overline{H_p} = \frac{-\sum_{i=1}^{N-1} q_k \log q_k}{logN} \tag{28}$$

From the perspective of signal complexity analysis, the power spectrum entropy can reflect the complexity of the signal energy under the power spectrum division. The simpler the signal is, the more concentrated the power spectrum energy distribution is, the smaller the power spectrum entropy is; the more complex the signal is, the more dispersed the power spectrum energy distribution is, the larger the power spectrum entropy is. For the special communication emitter signal, its fingerprint features affect the energy distribution of the power spectrum. Therefore, to a certain extent, we can use the power spectrum entropy to extract the nonlinear fingerprint features of the signal in the power spectrum domain.

2.3. Classifier Design. In machine learning methods, a large number of classifiers can be used for multiple classification tasks. The proposed algorithm in this paper uses the entropy feature vectors of the signal's different domains to analyze its nonlinear fingerprint features, which is originally a nonlinear classification problem. SVM is a classical machine intelligence algorithm based on the statistical learning theory, which is popular in multiple classification tasks. The classical model of SVM is a two-class classification model, which is defined as a linear classifier with a maximum interval on the feature space. It can also act as a nonlinear classifier when it encounters some linear inseparable problems. The core idea is using the suitable kernel function to map a linearly inseparable problem into a linearly separable problem in a high-dimensional space. In space, a separating hyperplane with the largest margin can be found using the structural risk minimization principle [21]. When the data are inseparable, the classification function is defined as

$$f(x) = \text{sign}\left[\left(\sum_{i=1}^{L} a_i y_i K\left(x_i, x_j\right)\right) + b\right], \tag{29}$$

where $K(x_i, x_j)$ is the kernel function, sign $(.)$ is the symbolic function, a_i is the ith mode embedded dimension, and y_i is the ith label. Detailed information about SVM can be found in [21].

In this paper, we use Python3.8 as an interpreter in PyCharm 2021 for classification experiments. There are three classes for the classification problems in the SVM from sklearn, they are LinearSVC, NuSVC, and SVC. In this task, we select SVC as the SVM classifier which is suitable for the linear inseparable problem. In the SVC, we choose the default Gaussian kernel as the kernel function and select the appropriate penalty coefficient c and kernel function parameter gamma by taking cross-validation. As shown in Tables 1 and 2, we select the penalty coefficient c as 10 and the gamma as 150 for the experiment. The parameter "multiclass" includes one-versus-one and one-versus-all. Since the one-versus-one technique has better performance and is more suitable for practical use [22], we adopt it in this paper. The training set and test set are randomly divided in the ratio of 6 : 4. The experiments are repeated 50 times, and the average value of 50 experiments is taken as the final result.

Table 3: The computational complexity of the multidimensional entropy algorithms.

Algorithm	Computational complexity
MPE	$O(N-(m-1)\tau) + O(N * m \log m) + O(nk)$
MApEn	$O(N^2)$
MJE	$O(N^2 + 5N)$

Table 4: Under different signal lengths, the recognition rate of this method.

	$K = 3$	$K = 4$	$K = 5$
200	52.33%	49.87%	41.68%
400	70.23%	69.42%	60.72%
600	86.54%	85.48%	82.70%
800	95.65%	93.32%	91.17%
1000	97.56%	97.37%	97.01%
2000	98.73%	98.63%	98.54%

2.4. CEEMDAN-MJE Algorithm Summary. The nonlinear fingerprint of the radio emitter has different performances in different domains. In the time domain, the nonlinear features of the signal are hidden in the complex signal waveform, which affects the signal singular spectrum subspace distribution. In the frequency domain, the nonlinear features of the signal also affect the power spectrum energy distribution, so we first adopt the CEEMDAN method to decompose the signal into multiple IMF components in different frequency ranges, which reduces the complexity of the signal in each domain and also facilitates to analyze the properties of the signal in each frequency range. By analyzing the 3-dimensional differential approximate entropy, singular spectral entropy, and power spectral entropy extracted from some IMF components to form a 5-dimensional multidomain joint entropy feature, the nonlinear fingerprint of the radio emitter is extracted in multiple domains. The specific steps of the proposed method are as follows (Algorithm 1). The parameters involved in the algorithm and the specific process of signal preprocessing are discussed in the next section.

3. Experiment Results and Analysis

3.1. Data Acquisition and Setup. To verify the robustness of the proposed method, the experiment is carried out using the USRP dataset and the public dataset. The transmit signals of five N210 USRPs were collected in a laboratory confined space. The distance between the transmitter and the

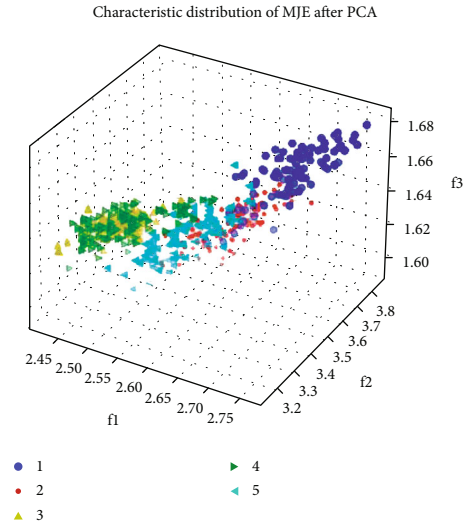

Figure 9: $L = 200$ distribution of MJE after PCA.

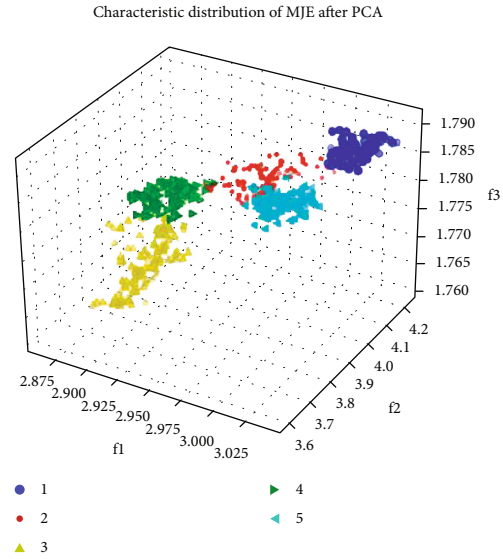

Figure 10: $L = 800$ distribution of MJE after PCA.

receiver is 10 m, and there are obvious obstacles between them. The signal modulation method is unified by 8QAM. The sampling frequency is 5 MHz, and the carrier frequency is 1G Hz. The signal of each type of radio emitter is 10^7 magnitude IQ sample points, and the collected data frame is 5000 points/frame. In this paper, the 100000 IQ sample points are selected for each type of USRP, and the transient part in each frame is removed at first. Then, we extract the time envelope of the IQ signal, taking 1000 sample points as a sample and 100 samples for each type of USRP. From the experiment result, it is clear that the time-domain envelope of the signal is intricate and cannot be identified from the time domain only. Therefore, this paper uses the CEEMDAN-MJE method to extract features from the different domains of the signal. Finally, we use the Northeastern University public dataset to verify the classification effect of the proposed method in the 16-class dataset. Next, we discuss the four parts of the study, namely, experimental parameters, computational complexity analysis, sample length analysis, and the noise robustness of the proposed method.

3.2. Experimental Parameters. In the CEEMDAN-MJE method, the most important parameters are the choice of IMF and the multidomain joint entropy hyperparameters. After the envelope of the signal is passed through CEEMDAN, multiple IMF functions are generated. From Figures 4 and 5, it can be seen that IMF2, IMF3, and IMF4 are the high- and medium-frequency parts of the signal and have obvious differences from each other, so we select these three IMFs to extract the nonlinear features. In [8], it is known that the extracted nonlinear features are most obvious when the value of m is from 2 to 10 and $r = 3$. Since the IMF component of the signal is more complex, this paper uses the three-dimensional difference approximation entropy [7–9] for a nonlinear analysis of the IMF. In the singular spectrum entropy feature extraction, the time delay constant τ is usually taken as 1 and the phase space embedding dimension σ is taken as 200. Through the multidomain

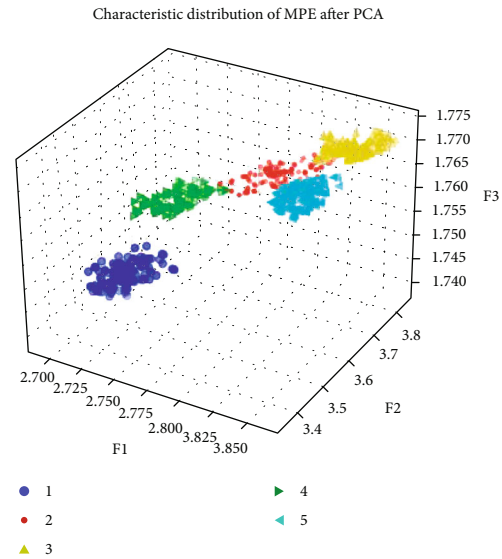

Figure 11: $L = 1000$ distribution of MJE after PCA.

joint entropy feature extraction, we could extract the rich nonlinear components in the original signal. So it can contain a variety of nonlinear RF fingerprint information, and the feature vector composed is more conducive to the subsequent recognition task.

3.3. Computational Complexity Analysis. The computation of the method is mainly concentrated on the MJE. This section analyzes the computational complexity of the MJE and several common entropy features. In [8], the computational complexity of the MApEn is about $O(N^2k - \tau\sum_{i=1}^{k} m_i)$. In MdApEn, the complexity is about $O(N^2k - \tau\sum_{i=1}^{k} m_i) + O(k\sum_{i=1}^{k} m_i)$. Due to $N \gg \max\{\tau, k, m_i\}$, the complexity can be simplified to $O(N^2)$. In SSE, it could need $N - (\sigma - 1)\tau$ addition operations from (18), and according to (19)-(22), the calculation is about $O(M)$ $(M = N - (\sigma - 1)\tau)$. The computational

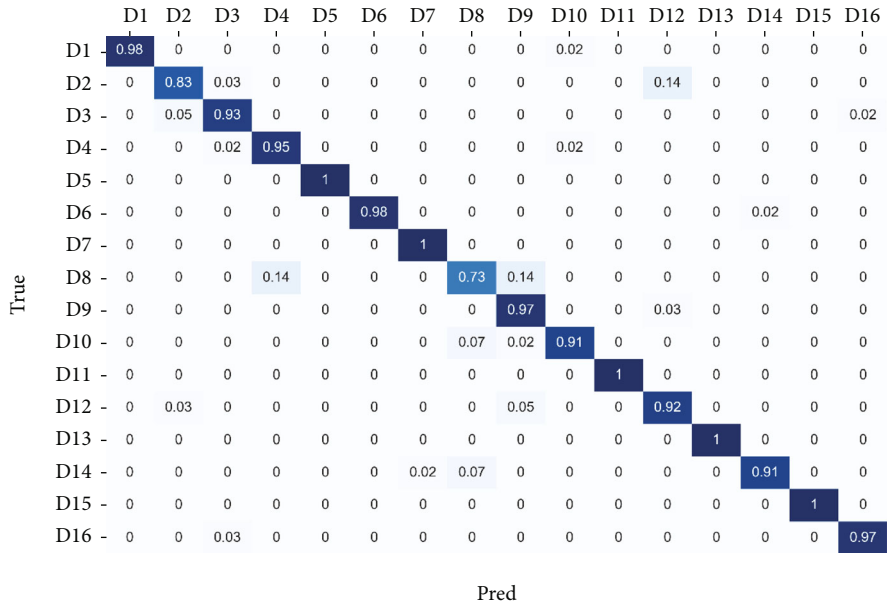

Figure 12: The confusion matrix of the 16-class radio emitter.

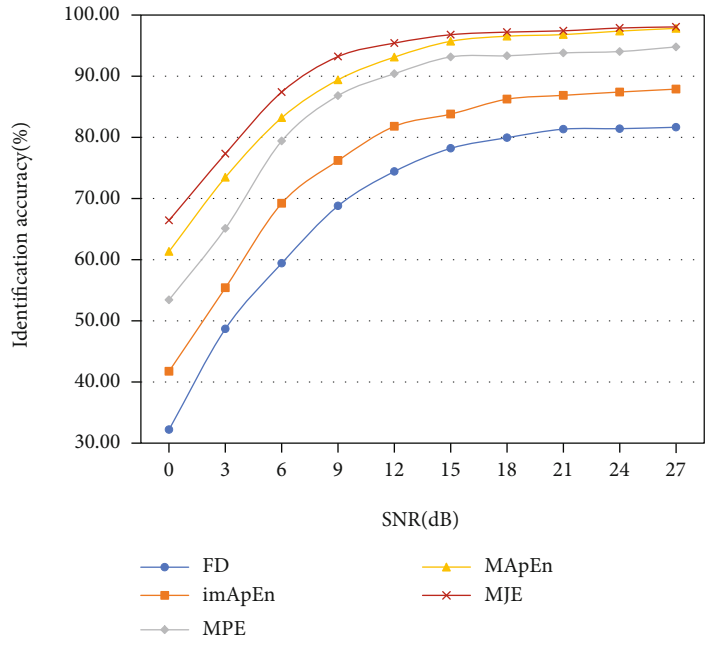

Figure 13: Identification performances under the AWGN channel.

complexity of SSE is about $O(2N)$. In PSE, it could need $2(N-1)$ addition operations from (23), and according to (25)-(26), the calculation is about $O(N-1)$. The computational complexity of PSE is about $O(3N)$. Therefore, the total computational complexity of the MJE is about $O(N^2+5N)$. In [6], the complexity of the multidimensional permutation entropy is about $O(N-(m-1)\tau)+O(N*m\log m)+O(nk)$, where n is dimensional of the permutation entropy and k is the number of the arrangement ways. In general, $N \gg \{m, k, n, \tau\}$. Therefore, the computational complexity of common algorithms is summarized in Table 3. The complexity of MJE is slightly higher than that of the MApEn, but it analyzes the nonlinear fingerprint of the signal from different domains. It is possible to extract more complete nonlinear features, which is beneficial to SEI technology. As shown in Table 3, the complexity of the MJE is mainly affected by the sample length, so we next analyze the choice of the sample length.

3.4. Sample Length Analysis. In the process of multidomain joint entropy extraction, the length of the signal sample

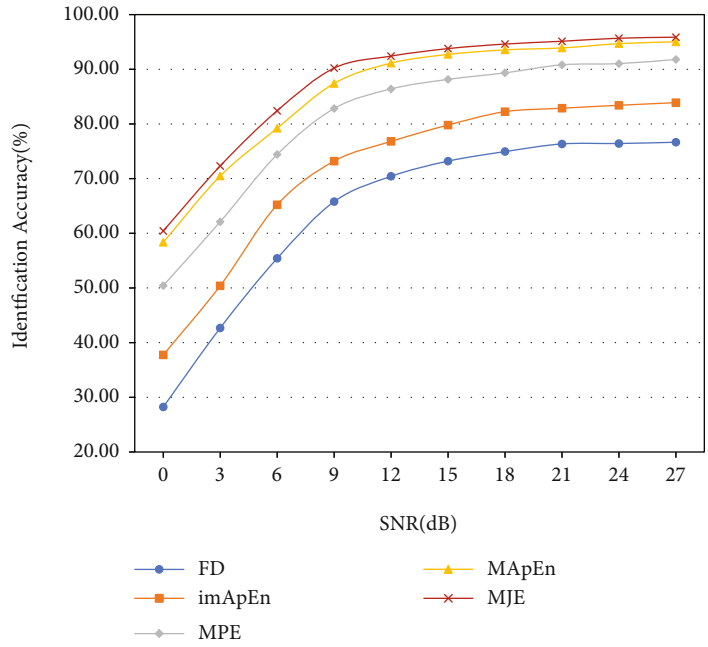

Figure 14: Identification performance under the Rayleigh fading channel.

has a great influence on the analysis of its entropy features. Theoretically, the longer the length of the signal, the more comprehensive the nonlinear features it contains. Therefore, within a certain range, increasing the length of the signal is beneficial to the study of signal identification. However, as the length of the sample signal increases, it not only increases the amount of experimental data but also increases the cost of computing. Therefore, this paper finds out the trend of the recognition rate with the length of the signal in the multiclassification problem through experimental comparison and provides a basis for the selection of the next sample length.

This time, the 5-class USRP dataset was selected, and the USRPs were named W1-W5. The IQ data of each USRP was taken out and divided according to 200, 400, 600, 800, 1000, and 2000 points per sample, and 100 samples were selected for each type of USRP. $K = 3$, 4 and 5 categories of the signal are selected for recognition experiments, and for $K = 3$, W1, W2, and W3 are selected; for $K = 4$, W1, W2, W3, and W4 are selected; and for $K = 5$, all categories are selected. In the signal recognition stage, the SVM classifier is selected. The training and test sets are randomly divided according to the ratio of 6 : 4. The experiments are repeated 50 times, and the average value of 50 experiments is taken as the final result. The recognition results obtained for different signal lengths are shown in Table 4.

As can be seen from Table 4, the length of the signal and the number of radio emitters have a great influence on the recognition rate of the experiment. As far as the length of the signal is concerned, the recognition rate increases more obviously when the number of sample points changes from 400 to 800, with an average increase of about 23%, while the recognition rate increases more slowly when it increases from 800 to 2000, with an average increase of only 3%. It can be seen that the longer the length of the signal, the more distinguishable the extracted fingerprint features are. To facilitate visualization, we reduce the 5-dimensional feature vector to 3-dimensional through principal component analysis (PCA). The PCA is a dimensionality reduction technique widely used in machine learning, which could extract the important components of the signal. Detailed information about PCA can be found in [23]. As shown in Figures 9–11, the distribution of different clusters represents the different radio emitter signals. Therefore, multidomain joint entropy needs samples of sufficient signal length. Too short samples are not enough to characterize the nonlinear features of its overall signal, and too long samples increase the computational cost. For the number of radio emitters, the recognition rate decreases with the same number of sample points when the number of radio emitters increases. This result is also consistent with the actual situation; when the number of radio emitters increases, the nonlinear features between each type of signal are less and less distinguishable in different domains. We need to increase the number of sample points, which enriches the nonlinear fingerprint features it contains. Therefore, the fingerprint features represented by MJE are more distinguishable.

Through the above analysis, on the 5-class USRP dataset, this paper uses 1000 data points per sample for the individual radio emitter identification task, and finally, only 100000 data points are used for each type of radio emitters, and the identification rate reaches more than 97%. If 2000 data points per sample are used for the experiment, the recognition rate is as high as 98.5%. To further verify the effectiveness of the method, this paper uses a Northeastern University public dataset of 16 classification problems, using

1000 sample points per sample and using 100,000 data points per type of radio emitter. The recognition rate reached 94.7%, and the confusion matrix results are shown in Figure 12. Let a_{ij} be the ith row and jth column of the confusion matrix, a_{ij} represents the probability that the emitter D_i is identified as the emitter D_j. Therefore, the confusion matrix further illustrates the effectiveness of the method for multiple types of radio emitter.

3.5. Noise Robustness of the Method. To evaluate the noise robustness of the proposed method, a series of controlled experiments are conducted in this paper using the USRP dataset. Four other different techniques based on steady-state entropy feature extraction were used in the experiments, and classification experiments were performed under the same conditions: (1) fractal dimension [24] (box dimension and information dimension); (2) multidimensional permutation entropy features [6], (3) improved approximate entropy features [7]; and (4) multidimensional approximate entropy features [8]. To ensure the fairness of the comparison, all features were preprocessed by the CEEMDAN algorithm before extraction, and the experiments were conducted under the same conditions. To further evaluate the noise robustness of the proposed method, we choose the Gaussian channel and Rayleigh fading channel to add different noises to the original signal and analyze the performance of different methods in the range of 0-25 dB SNR.

In the Gaussian channel, it can be seen from Figure 13 that using multidimensional entropy such as MPE, MApEn, and MJE to analyze the signal has a better recognition effect compared with one-dimensional entropy, which shows that the multidimensional entropy analysis method can extract more accurate nonlinear fingerprint information. The method in this paper further analyzes the entropy features in different domains of the signal that is different from the existing methods, and the experiments show that the multidomain joint entropy features have better recognition performance. Therefore, compared with the existing methods, the MJE method has greater advantages in extracting the nonlinear fingerprint features. To further evaluate the noise robustness of the method, the classification effect of the original signal under the influence of the Rayleigh fading channel is investigated in this paper. As can be seen from Figure 14, the recognition rate of the amplitude source signal in the Rayleigh fading channel environment is slightly lower than that in the Gaussian channel, because the fading coefficient α in the Rayleigh fading channel leads to greater randomness, blurs the fingerprint differences between radio emitters, and increases the difficulty of nonlinear feature extraction. But the nonlinear analysis of it from multiple domains can reduce the influence brought by its randomness and effectively extract the nonlinear fingerprint features of the signal. According to the above analysis, the method in this paper can achieve more than an 85% recognition rate in an environment above 5 dB SNR. It also has great noise robustness performance, which is better than other nonlinear feature extraction methods on the USRP dataset.

4. Conclusion

This paper is devoted to the study of individual identification of communication radio emitters by extracting the nonlinear fingerprint of communication signals. Since the nonlinear RF fingerprints have a complex generation procession, considering the large of nonlinear features in different domains, the signal is studied by nonlinear analysis in multiple domains. Considering more channel and environmental noise interference in the actual signal, which adds a lot of channel noise to the signal, the CEEMDAN algorithm is performed first, which reduces the influence of noise on the original signal. Then, the multidomain joint entropy features of the IMF of high-frequency components are extracted. Finally, a high recognition rate is achieved by the SVM classifier. Therefore, the multidomain joint entropy is beneficial to the analysis of its nonlinear fingerprint features. After the experimental research shows that the proposed method has good noise robustness performance and can achieve more than 85% recognition rate above 5 dB SNR. It also has good robustness in large numbers of radio emitters and can achieve a 94.7% recognition rate on the 16-class public dataset, so the CEEMDAN-MJE method is suitable for the individual identification of communication radio emitters in the case of multiple numbers and above 5 dB SNR. The Northeastern University public dataset download address is as follows: https://http://genesys-lab.org/oracle.

Data Availability

The Northeastern University public dataset (dataset#1) used to support the findings of this study is available from the corresponding address: https://genesys-lab.org/oracle. The 5-classified USRP dataset used to support the findings of this study has not been made available because there is some secret parameter information in the experimental data.

Conflicts of Interest

The authors declare that they have no known competing financial interests or personal relationships that could have appeared to influence the work reported in this paper.

References

[1] X. Dan, *Research on mechanism and methodology of Specific emitter identification [D]*, National University of Defense Technology, 2008, [Ph.D. dissertation].

[2] A. E. Spezio, "Electronic warfare systems," *IEEE Transactions on Microwave Theory and Techniques*, vol. 50, no. 3, pp. 633–644, 2002.

[3] O. Ureten and N. Serinken, "Wireless security through RF fingerprinting," *Canadian Journal of Electrical and Computer Engineering*, vol. 32, no. 1, pp. 27–33, 2007.

[4] T. L. Carroll, "A nonlinear dynamics method for signal identification," *Journal of Nonlinear Science*, vol. 17, no. 2, p. 023109, 2007.

[5] Y. Yuan, Z. Huang, F. Wang, and X. Wang, *Radio specific emitter identification based on nonlinear characteristics of signal*

[C], IEEE International Black Sea Conference on Communications and Networking. IEEE, 2015.

[6] S. Deng, Z. Huang, X. Wang, and G. Huang, "Radio frequency fingerprint extraction based on multidimension permutation entropy," *International Journal of Antennas and Propagation*, vol. 2017, 6 pages, 2017.

[7] Y. Xie and S. Wang, *Specific emitter identification based on nonlinear complexity of signal*, [C] IEEE International Conference on Signal Processing, Communications and Computing (ICSPCC), 2018.

[8] L. Sun, X. Wang, A. Yang, and Z. Huang, "Radio frequency fingerprint extraction based on multi-dimension approximate entropy," *IEEE Signal Processing Letters*, vol. 27, pp. 471–475, 2020.

[9] Y. Li, X. Gao, and L. Wang, "Reverse dispersion entropy: a new complexity measure for sensor signal," *Sensors*, vol. 19, no. 23, p. 5203, 2019.

[10] M. E. Torres, M. A. Colominas, G. Schlotthauer, and P. Flandrin, *A complete ensemble empirical mode decomposition with adaptive noise*, 2011 IEEE International Conference on Acoustics, Speech and Signal Processing (ICASSP), 2011.

[11] N. E. Huang, Z. Shen, S. R. Long et al., "The empirical mode decomposition and the Hilbert spectrum for nonlinear and non-stationary time series analysis [C]//The Royal Society A," *Mathematical Physical & Engineering Sciences*, vol. 454, no. 1971, pp. 903–995, 1998.

[12] "Xiao Hui Rong. Research on analytical methods of mutation components in time-varying signals [M]," *Harbin Institute of Technology*, 2020.

[13] X. Yang, G. Cheng, and H. Liu, "Improved empirical mode decomposition algorithm of processing complex signal for IoT application," *International Journal of Distributed Sensor Networks*, vol. 2015, 8 pages, 2015.

[14] W. Zhaohua and N. Huang, "Ensemble empirical mode decomposition: a noise-assisted data analysis method [J]," *Advances in Adaptive Data Analysis*, 2009.

[15] J. R. Yeh, J. S. Shieh, and N. E. Huang, "Complementary ensemble empirical mode decomposition: a novel noise enhanced data analysis method," *Advances in Adaptive Data Analysis*, vol. 2, no. 2, pp. 135–156, 2010.

[16] Y. Li, Y. Li, X. Chen, J. Yu, H. Yang, and L. Wang, "A new underwater acoustic signal denoising technique based on CEEMDAN, mutual information, permutation entropy, and wavelet threshold denoising," *Entropy*, vol. 20, no. 8, p. 563, 2018.

[17] N. Soltanieh, Y. Norouzi, Y. Yang, and N. C. Karmakar, "A review of radio frequency fingerprinting techniques," *IEEE Journal of Radio Frequency Identification*, vol. 4, no. 3, pp. 222–233, 2020.

[18] Steve Pincus and Wei Min Huang, "Approximate entropy: statistical properties and applications," *Statistics*, vol. 21, no. 11, pp. 3061–3077, 1992.

[19] H. S. Kim, R. Eykholt, and J. D. Salas, "Nonlinear dynamics, delay times, and embedding windows," *Physica D: Nonlinear Phenomena*, vol. 127, no. 1-2, pp. 48–60, 1999.

[20] J. Jiang, *Research on real-time signal measurement technology based on information entropy and its application [D]*, University of Electronic Science and Technology of China, 2017.

[21] J. C. B. Christopher, "A tutorial on support vector machines for pattern recognition," *Data Mining and Knowledge Discovery*, vol. 2, no. 2, pp. 121–167, 1998.

[22] K. R. Müller, S. Mika, G. Rätsch, K. Tsuda, and B. Schölkopf, "An introduction to kernel-based learning algorithms," *IEEE Transactions on Neural Networks*, vol. 12, no. 2, pp. 181–201, 2001, s.

[23] J. Shlens, *A tutorial on principal component analysis*, 2014.

[24] J. Dudczyk and A. Kawalec, "Fractal features of specific emitter identification," *Acta Physica Polonica A*, vol. 124, no. 3, pp. 406–409, 2013.